Mode I cracking of three tropical species from Cameroon: the case of bilinga, dabema, and padouk wood

Rosmi Biyo'o, Achille Bernard Biwole, Rostand Moutou Pitti, Charly Julien Nyobe, Benoit Ndiwe, Emile Jonathan Onana, Emmanuel Yamb

▶ **To cite this version:**

Rosmi Biyo'o, Achille Bernard Biwole, Rostand Moutou Pitti, Charly Julien Nyobe, Benoit Ndiwe, et al.. Mode I cracking of three tropical species from Cameroon: the case of bilinga, dabema, and padouk wood. Wood Material Science and Engineering, inPress, ⟨10.1080/17480272.2024.2314750⟩. ⟨hal-04617275⟩

HAL Id: hal-04617275

https://hal.science/hal-04617275v1

Submitted on 19 Jun 2024

HAL is a multi-disciplinary open access archive for the deposit and dissemination of scientific research documents, whether they are published or not. The documents may come from teaching and research institutions in France or abroad, or from public or private research centers.

L'archive ouverte pluridisciplinaire **HAL**, est destinée au dépôt et à la diffusion de documents scientifiques de niveau recherche, publiés ou non, émanant des établissements d'enseignement et de recherche français ou étrangers, des laboratoires publics ou privés.

HAL Authorization

Mode I cracking of three tropical species from Cameroon: the case of dabema, bilinga and padouk wood

Rosmi Biyo'o Biyo'o[1*], Achille Bernard Biwole[1], Rostand Moutou Pitti[3,4], Charly Julien Nyobe[2], Benoit Ndiwe[1,2], Emile Jonathan Onana[1], Yamb Emmanuel[1,2]

[1]University of Douala, Advanced Teacher's Training College for Technical Education, Engineering Sciences Doctoral Training Unit, Laboratory of Forest and Wood Resources Valorisation, P.O. Box, 1872 Douala, Cameroon

[2]University of Douala, Advanced Teacher's Training College for Technical Education, Engineering Sciences Doctoral Training Unit, Laboratory of Mechanic, P.O. Box, 2701 Douala, Cameroon

[3]Université Clermont Auvergne, CNRS, Institut Pascal, BP 10448, F-63000 Clermont-Ferrand, France

[4]CENAREST, IRT, BP14070, Libreville, Gabon

*Corresponding author: Biyo'o Biyo'o Rosmi. Email: rosnybiyo@gmail.com

ORCID ID

Achille Bernard Biwole: https://orcid.org/0000-0003-3964-771X
Rostand Moutou Pitti: https://orcid.org/0000-0002-4596-4693
Charly Julien Nyobe: https://orcid.org/0000-0002-5343-8773
Benoit Ndiwe: https://orcid.org/0000-0003-0692-0353

Abstract:

This work aim to study the initial stress to cracking of Cameroonian tropical woods. The forests of the Cameroonian part of the Congo Basin (*CB)*, abound in species highly sought after for structural applications. However, very little information is available on the Mode I cracking of these wood species. Specimens of sound wood from Dabema (*Piptadeniasmetrum africanum)*, Padouk (*Pterocarpus soyauxii Taub*) and Bilinga (*Diderrichii nauclea*) were produced. These specimens were subjected to three-point bending tests. Physical (density and moisture content), mechanical (modulus of elasticity, bending stress at break) and energetic (restitution rate and stress intensity factor) properties were determined. The results gave a restitution rate of 581.11 j/m² for *Dabema*, 519.72 j/m² for Bilinga and 201.61 j/m² for *Padouk*, and a stress intensity factor of 0.98 MPa*$m^{1/2}$ for Dabema, 1.28 MPa*$m^{1/2}$ for Bilinga and 1.0 MPa*$m^{1/2}$ for *Padouk*. It can be seen that *Dabema* and *Bilinga* are more resistant to crack propagation than *Padouk*. On the other hand, *Bilinga* and *Padouk* absorb much more of the energy that causes micro cracks than Dabema.

Key words: energy restitution rate, mode I, cracking, tropical woods

Introduction

The Congo Basin (*CB) forest* cover*s* almost 243 million hectares, accounting for a quarter of the world's tropical forest area(CIFOR 2014). These forests are spread across many African countries, including Cameroon, the Central African Republic, the Republic of Congo, the Democratic Republic of Congo, Gabon and Equatorial Guinea. The *CB* forests contribute to combating the greenhouse effect by absorbing carbon from the air. In each of these countries, the forest ecosystems are home to an exceptional biodiversity of trees, flora and fauna. By way of illustration, around 600 tree species have been inventoried in the Cameroonian part of the CB (FAO 2006). These woods are used in various construction applications, including parquet flooring, light and heavy timber frames, shipbuilding, bridges and railway sleepers. Despite their enormous potential *in constructing* structures, the technological properties of *CB*'s wood species are still little known by players on the international tropical timber markets. (Ravenshorst et al.,2013). The mechanical behavior of these species, specifically their fracture properties, remain poorly studied in the literature, which hinders the reliable design of such structures. This can lead, for example, to the sudden failure of structures, which is unacceptable and reduces their competitiveness and potential to be valued in international markets. It is, therefore, essential to carry out further studies to provide the missing properties such as cracking behavior.

Numerous studies have been conducted to evaluate fracture characteristics and their effects on timber constructions (Jungstedt et al. 2022, Romanowicz 2022,Yu et al. 2021). Toughness, the material's ability to resist crack propagation, is a fundamental property for characterizing a wood species (Yin et al. 2023, Zhu and J**oyc**e 2012, Mall et al. 1983). It is influenced by temperature, growth habit and relative humidity (RH) (Kurul and Görgün 2022, Bertolin et al. 2021, Hassan and Brabec 2023, Merhar and Pitti 2023, Reiterer and Tschegg 2002).

The type of methods developed on identifying systems and detecting cracks in brittle materials have been carried out. These methods are divided into two general categories including destructive and non-destructive identification. Destructive methods using structural sampling examine the extent of cracks or even failures in material specimens. Non-destructive methods are also divided into local and general. Many researchers have used destructive methods based on linear elastic fracture mechanics to study the fracturing mechanism of concrete and rock structures (Ding and Lu 2016, Gomes et al. 2018). Methods based on the examination of the vibrational (dynamic) properties of a structure to detect and estimate possible cracks (Benedetti et al. 2018). For example, several experimental and numerical studies have been devoted to explaining the fracture and damage

mechanisms of rock and concrete structures (Fu et al. 2022, Fu et al. 2021, Zhou et al. 2022, Fu et al. 2023, Wang et al. 2023)

Currently, in the literature, some authors maintain that wood cracking is strongly linked to its anatomical structure by considering the orthotropic morphology of wood. A closer look at the microstructure of wood reveals other features, such as growth rings, sap channels and radial channels (Moura and Dourado 2018, Ostapska and Malo 2020), which affect the mechanics of crack propagation in wood.

Maaß et al. (2020) showed that wood is a highly anisotropic structure that generates resistant interfaces and deflects and localizes cracks at these interfaces (Zhang et al. 2018). In addition, the velocity is highly sensitive to the fibre angle. On the other hand, other authors maintain that wood cracking is strongly linked to its density (Odounga et al. 2018, Odounga et al. 2019). Healthy specimens of *Iroko* and *Okum*e were subjected to tensile tests and it was found that the fracture toughness of *Iroko* is higher than that of *Okume*. Nziengui et al. (2018) showed that for similar densities, the results of the various comparative analyses indicate*d* no significant differences between the parameters highlighted in this study for these species despite the difference in their growth zones.

Other authors maintain that the acceleration of cracks and their propagation depend on the variation of the water content in the wood (Dourado et al. 2015, Engonga Edzang et al. 2021, Forsman et al. 2021, Phan et al. 2017). Despite numerous partial studies, there is no comprehensive study in the literature that links a number of factors and their influence on the fracture properties of tropical woods simultaneously. Therefore, this study aims to investigate the overall influence of different factors on the mode I (bending) fracture properties of Dabema, Bilinga and Padouk timbers, both for different crack lengths, different species, different basal density rate and, for the direction of tissue loading (longitudinal-tangential). Studying the fracture properties of tropical woods from Cameroon is crucial to guiding local engineers in their choice of construction materials and supporting local populations in their choice of construction materials other than concrete and steel.

This study aims to examine the fracture behavior of species produced in Cameroon, such as Bilinga (*Diderrichii nauclea*), Dabema (*Piptadeniasmetrum africanum*) and Padouk (*Pterocarpus soyauxii Taub*). This knowledge will represent an important step towards the optimal use of these species for structural applications. The design of such structures requires detailed understanding of the mechanical behavior of the constituent material, particularly with regard to cracking. This phenomenon precedes the final ruin of the structure. As such, it deserves special attention.

Materials and methods

Equipment

In this study, three species of wood were sampled, namely Bilinga (*Diderrichii nauclea*), Dabema (*Piptadeniasmetrum africanum*) and Padouk (*Pterocarpus soyauxii Taub*), each with a diameter of 77-92 cm, within the Unité Forestière d'Aménagement (UFA) of the Bonaberi district, Wouri department, coastal region. Logs (Figure 1) were taken from each timber. These logs were sawn into quarters and then cut into the dimensions required for the various tests. Flawless wood samples were taken randomly from the sections obtained to determine the physical, mechanical and energetic properties. The samples were conditioned in a shed at room temperature and stored under these conditions for a month until they were tested. The study focuses on these three Central African tropical woods, given their great commercial importance and use in Figure 1.

Experimental methods

Physical properties

Water content

To measure moisture content (TH), 20 samples (2 cm x 2 cm x 2 cm) per species were prepared and stored in polyethylene bags to prevent moisture loss after initial weighing. They were then dried in an oven at 103°C until a constant mass was obtained. Moisture content is defined as the ratio of the mass of water contained in the wood to the anhydrous mass, according to standard (NF B51- 004. 1985). The water content of wood at a given moment is obtained using the following formula:

$$H = \frac{m_H - m_0}{m_0} \quad (1)$$

m_H mass of the test piece at humidity level h, in (g);

m_0 is the mass of the test piece in the anhydrous state, in (g) and H : water content, in (%)

Basal density

The basal density is the ratio of the anhydrous mass (M_0) to its volume in the saturated state (V_S) of the sample, French standard (NF B51-005. 1985) allows the basal density to be calculated using the formula :

$$D_b = \frac{M_0}{V_S} \quad (2)$$

Where (D_b)= g /cm ,^{3} M_0 in g and V_S in cm^3

Determination of mechanical properties

The longitudinal modulus of elasticity and breaking stress are determined by the three-point bending test in accordance with standard (NF B51 - 008. 2017). Figure 3 shows the experimental setup used to perform the test. The machine is equipped with two comparators.

The modulus of elasticity (E_f) was calculated based on the principles of standard N F B 51-016 (1987). It is a function of load, displacement and stiffness coefficient. By recording the force-deflection curve, the bending stiffness K can be calculated within the linear zone:

$$K = \frac{\Delta F}{\Delta f} \tag{3}$$

The modulus of elasticity (E_f), expressed in (MPa) or (N/mm^2) will be determined using the following equation:

$$E_f = \frac{L^3}{4bh^3}\left(\frac{\Delta F}{\Delta f}\right) = \frac{L^3}{4bh^3}(K) \tag{4}$$

With E_f: modulus of elasticity in (MPa); ΔF: variation in the load applied until failure (N); Δf L: is the distance between the axes of the supports (mm); b: is the measured with of the specimen (mm); h: is the measured height of the specimen (mm)**.**

Knowing the maximum braking force, we can obtain the breaking stress from the classic beam theory formulae

$$\sigma_n = \frac{3SP}{2BW^2} \tag{5}$$

Where B and W are, respectively, the width and thickness of the beam, S is the span of the beam and P is the load.

Energy properties

Nominal bending stress

Using the equation (5), the nominal stress on the specimens without primer and with primer of 4 and 8mm was calculated.

The following equation was used to calculate fracture toughness (ASTM E399-09, 2009)

Stress intensity factor

The energy properties (energy restitution rate, stress intensity factor and bending stress) of the SENB specimens were defined as follows: L = 360 mm, a = 20 mm and b = 20 mm. A total of 15 specimens per species were subdivided into three blocks: 05 specimens with no defect, 05 specimens with a defect 4 mm deep on the axis and 05 specimens with a defect 8 mm deep.

Three energy parameters were obtained from the P-δ curves, namely the stress intensity factor (K_{IC}), nominal bending stress (σ_n) and specific energy at failure (Gf). Figure 4 shows a schematic diagram of the three-point SENB test.

According to the theory of linear fracture mechanics, the stress intensity factor K_I of mode I is calculated as follows:

$$K_{Ic} = \sigma_n \sqrt{\pi a} f(\frac{a}{W}) \quad (6)$$

Where f(a/W) is the crack geometry factor.

Fracture is initiated when K_I reaches the critical stress intensity factor, which is obtained by substituting the critical nominal stress *from* the nominal stress in equation (6) (Gross, B., & Srawley 1965) derived a relationship f(a/W) -a/W for an isotropic material as follows:

$$f(\frac{a}{W}) = 1.09 - 1.735(\frac{a}{W}) + 8.20(\frac{a}{W})^2 - 14.18(\frac{a}{W})^3 + 14.57(\frac{a}{W})^4 \quad (7)$$

Energy restitution rate

The fracture toughness Gic ($J.m^{-2}$), which represents the work required to separate the fracture surfaces, was calculated from the integrated area under the P-δ curve; divided by the fracture surface area using the following formula (Arif C Konukcu, Katip, and Universitesi 2022; Majano Majano, Hughes, and Fernández-Cabo 2010; Grandgirard et al. 2002) :

$$G_{IC} = \frac{1}{(W-a) \times B} \int_0^{\delta \max} P(\delta) d\delta \quad (8)$$

Where a is the crack length at the origin, *P* is the load, *δ* is the deflection at the loading point, and $(W-a) \times B$ is the fracture surface area.

Statistical analysis

Data obtained from physical and mechanical properties measurements were first subjected to descriptive statistics to calculate means and standard deviation. Discriminant analysis was used to describe the influence of leader length on the energetic properties of wood cracking and the variation in energetic parameters between the three tropical woods. An analysis of variance (ANOVA) and Students' paired test were used to check that the mean values obtained varied significantly between the species. The results were considered significant at the $p < 0.05$ confidence level.

Results and discussion

Physical properties

Table 1 shows the average values for the physical properties of Dabema, Bilinga and Padouk wood. The moisture content values obtained for the different species are 19.14% for Padouk, 22.1% for Bilinga and 25.63% for Dabema. This indicates that the different species concentrate a large quantity of free water a few months after felling, which could affect the dimensional stability of the wood and favour the growth of bio degraders (Boadu et al. 2017). Therefore, timber should be carefully dried before being used in a timber structure to avoid problems associated with high moisture in the wood (Gérard et al. 1998), which could destroy its structural rigidity in service. The minimum and maximum moisture contents of the three tree species followed Simpson's (1991) results, which stated that the moisture content of some species can be as low as 30% due to site variations and falling seasons.

Basal density is (0.73 ± 0.03) for Bilinga; (0,.83± 0.05) for Padouk and Dabema (0.69 ± 0.03). This could be due to the complex interactions between many factors, including forming an auxin gradient (Jozsa et al. 1994). The basal density values of the three species could be classified as medium-heavy wood, according to Gérard et al. (2017).

Mechanical properties

Table 2 shows the mean values of the mechanical properties of Dabema, Bilinga and Padouk wood. The mean values of modulus of elasticity (MOE) obtained for the different species ranged from 8392.31 to 9905.29 MPa. The bending stresses ranged from 66.94 to 89.82 MPa. Dabema, Bilinga and Padouk are medium-strength woods, as suggested by (Gérard et al. 2017).

Figure 5 shows typical load-deformation curves from tests carried out on specimens of different crack lengths. The observations generated show two distinct behaviors for the specimens tested: (i) linear behavior that increases until a sudden crack appears; (ii) ductile behavior. For the different specimens, Padouk showed stable crack propagation until specimen failure. Dabema and Bilinga behaved differently. After initiation of macro-cracking at maximum horizontal bending force a sudden drop in load-displacement curve occurred, indicating unstable crack propagation. The curves for Padouk wood show smoother and more uninterrupted behavior than those for Dabema wood and Bilinga wood, which show more unstable and scattered behavior after crack initiation. The explanation could be linked to the complex structure of Dabema and Bilinga (Figure 7), consisting of a high fraction of radially oriented cells (rays, fibre) acting as a reinforcement that forces the crack to take a more sinuous path (Maaß et al. 2020, Reiterer and Sinn 2002). The specimen with an 8mm

deep flaw lowered the maximum loads, as shown in Figure 5. The bending behavior shifted to reduce the maximum stress during the decrease.

Figure 6 shows that, depending on the fibre direction, it is even possible for more than one crack path to be created simultaneously at different propagating locations. It shows the typical failure modes of SENB test blocks cracking at the interface in the LT flexural crack propagation system. This is explained by Zhang et al. (2018), who also showed a high sensitivity of the speed to the angle of the fibers.

Energy parameters

Table 3 shows the mean values and results of the analysis of variance and Tukey test on the energy properties of three tropical woods, Bilinga, Padouk and Dabema. The energy restitution rate of Bilinga wood increases with increasing crack length. At crack lengths of 8mm and 4mm, the Gic(j/m²) restitution energy rate of Dabema (581.11 j/m²) was higher than that of Bilinga (519.79 j/m²) and Padouk (490.61 j/m²). This makes a significant difference after the comparison test between Dabema and Padouk. This can be explained by the anatomical structure of the woods (Moura et Dourado 2018, Ostapska et Malo 2020). The effect of anatomical structure and wood species on the rate of energy restitution was determined based on direct mean comparisons of the main effect. The average comparison results of the energy parameters for the wood species are summarized in Table 3. Arif Caglar Konukcu, Quin, and Zhang (2021) mentioned that a test specimen's mode I fracture behavior can be affected not only by its density but also by its microstructure.

The stress intensity factor increased with increasing crack length. Depending on the crack length of 8mm, the Gic restitution energy rate (j/m²) of Dabema (0.98 MPa*$m^{1/2}$) was lower than that of Bilinga and Padouk, which varied (1.10 to 1.28 MPa*$m^{1/2}$). The K parametric was not significant between the three woods. These results agree with Maria et al. (2010) work, which found crack length-dependent stress intensity factors for several wood species in her literature overviews. However, wood being an orthotropic material, the values cannot be homogeneous on the three-dimensional scale.

The results showed that Dabema and Bilinga have more ductile behavior, i.e. the rate of energy restitution is much higher with extended initiation specimens than Padouk. However, Padouk and Bilinga have a higher stress intensity factor than Dabema. This could be because the specific fracture energy is not independent of a species's loading mode or crack propagation system. Hence, it can be influenced by other parameters, such as density. Indeed, previous research has mentioned that wood's mode I fracture behavior can be affected by its density and microstructure (Frühmann 2002, Konukcu

et al. 2021), and that could explain why Dabema and Bilinga are more resistant to crack propagation due to their wavy and counter fiber orientation, as illustrated in Figure 7.
Because of the more straightforward structure of wood, a crack can take a relatively straight path, whereas the more complex structure of wood could force the crack to take a more circuitous route (Figure 6). In addition, fibre bridging could play an important role in energy dissipation during the crack propagation phase.

Figure 8 shows the mean, maximum and standard deviation of the fracture energy parameters obtained for the three specimen combinations with different crack lengths (A0 to A2). Varying cracking parameters, such as crack length and different wood species.

Figure 8 shows the results that were tested by ANOVA (Figure 3 and Figure 4), which are consistent with previous studies that found similar results for the influence of crack length on these fracture mechanics properties (Maria et al. 2010). The bending energy restitution rate of cracked specimens was significantly lower than that of a specimen without a crack, even when the crack was extremely short (Konukcu 2022, Konukcu et al. 2022, Luimes et al. 2018, Maria et al. 2010, Nakao et al. 2012, Reiterer & Sinn 2002, Stanzl-Tschegg 2006). The maximum load is evident through angular peaks, typical of linear elastic brittle hardwoods (Stanzl-Tschegg 2006). In addition, the rays consume additional fracture energy, which acts as reinforcement, creating fibre bridges behind the crack base as the crack propagates (Majano Majano, Hughes and Fernández-Cabo 2010). Reiterer and Sinn (2002) have pointed out that increased specific fracture energy increases ductility. The rate of energy restitution of a cracked specimen will approach the bending energy of a specimen without a crack when the crack length is reduced (Irwin 1958).

Table 4 shows the mean values and results of the analysis of variance and Tukey test on the energy properties of Bilinga, Padouk and Dabema wood. The influence of crack length on energy parameters. The rate of energy restitution (G_{IC}), the stress intensity factor (K_{IC}) and the bending stress of Dabema, Bilinga and Padouk timbers on specimens with different initiation depths for each timber. For Dabema wood, this table shows no significant difference between the (G_{IC}) of the first initiation value of a specimen and that of the third initiation value. On the other hand, this table shows a significant difference between the (G_{IC}) of the first and third boot values of Bilinga and Padouk wood. With regard to (K_{IC}) only the variation in the Padouk wood primers showed a significant difference.

Table 4 also shows the mean values of the bending stress for the three woods. This table shows a significant difference between the variation of the primers on each wood. The p-value of the comparison test is above the significance level of 0.05.

Impact of density (D_b) and primer variation (a_0) on energy restitution rate (G_{IC}) and stress intensity factor (K_{IC})

The histograms in Figure 9 show the evolution of the sample's energy restitution rate (Gic) after each wood at different priming levels.

Figure 9 compares the histogram, showing a decrease in the amplitude of the energy restitution rate (G_{IC}) with the different values of the baits. Between the first and third values of the primer depth of, a regression of G_{IC} of 177.45%, 236.60% and 503.67% for Dabema, Bilinga and Padouk This comparative regression of G_{IC} can be explained by the typical tangential structure of three wood species indicating the fibre orientation and microstructure of Padouk, Dabema and Bilinga (Figure7). Zhang et al. (2018) also show a high sensitivity of velocity to fibre angle. Figure 9 shows that Dabema has a higher GIC value when the initiation is higher than Padouk and Bilinga. This is explained by the anatomical structure of the wood, where Dabema has entangled fibres (Figure 6 and Figure 7).

Figure 10 shows the effect on the amplitude of the energy restitution rate *Gic* and the stress intensity factor *Kic* (their maximum values) of the Padouk, Bilinga and Dabema specimens as a function of the density of each species. (a_0) denotes the initial length

In general, for the three species studied, we observed a difference in the amplitude of the rate of energy restitution from the value of initiation (a_0 =4mm) on each species and the value of G_{IC} increases as a function of density. The G_{IC} of Padouk wood is higher than that of Bilinga and Dabema wood in the low-prime specimens. The high density of Padouk wood can explain this result. (Odounga et al. 2018, Rostand et al. 2019) showed that wood cracking is strongly linked to its density. The (G_{IC}) of Dabema and Bilinga wood are close together due to their similar density values.

Nziengui et al. (2018) showed that for similar densities, the results of the various comparative analyses indicate no significant differences between the parameters evaluated. With regard to (K_{IC}), Padouk wood has higher values than Bilinga and Dabema wood on the low-prime specimens. The higher density of Padouk wood can explain this.

Conclusion

This work aimed to study the fracture parameters of three tropical species from the Cameroon forest, namely Dabema (Piptadeniasmetrum africanum), Bilinga (Diderrichii nauclea) and Padouk (Pterocarpus soyauxii Taub). The physical properties (water content, basal density), mechanical properties (young's modulus, bending stress) and energy properties (energy restitution rate, stress intensity factor) were determined. The average values of the modulus of elasticity (MOE) obtained

for from the different species are between 8392.31 and 9905.29 MPa. The bending failure stresses are between 66.94 and 89.82 MPa. Dabema, Bilinga and Padouk are woods with medium mechanical resistance. The results show that the energy restitution rate for Dabema is 581.11 j/m², for Bilinga 519.72 j/m², and for Padouk 201.61j/m² and the stress intensity factor for Dabema 0. 98 MPa*$m^{1/2}$, for Bilinga 1.28 MPa*$m^{1/2}$, and for Padouk 1.10 MPa*$m^{1/2}$. The results show that Dabema and Bilinga have more ductile behavior, i.e., the rate of energy restitution is much higher than Padouk's. However, Padouk and Bilinga have a higher stress intensity factor than Dabema for this reason, Dabema and Bilinga are more resistant to crack propagation than Padouk.

On the other hand, Bilinga and Padouk absorb much more of the energy at the origin of microcracks than Dabema. However, the differences observed between the three woods studied show the need to extend the study of cracking behavior to other tropical woods. In this respect, African tropical woods stand out with some confidence, given their exceptional characteristics. Finally, in a global context marked by strong competition between wood and other construction materials, we will opt for a strategy of applying our results. All our results will be published as they become available. Dissemination will be open to all contractors and will not be restricted by any pressure group. What's more, if we are successful, the necessary developments that will accompany the industrial transfer to Cameroon will make better use of the diversity of tree species. In future studies, different loading modes and three-dimensional effects will also be taken into account using the Mixed Mode Crack Growth Specimen in order to better study the effect of scale and its impact on wood failure. The impact of moisture variation on the cracking parameters of this type of wood will also be investigated

Conflicts of interest

The authors declare that they have no conflicts of interest to report regarding the present study

References

Benedetti, Andrea, Giacomo Pignagnoli, and Mirco Tarozzi. 2018. "Damage Identification of Cracked Reinforced Concrete Beams through Frequency Shift." *Materials and Structures/Materiaux et Constructions* 51 (6). https://doi.org/10.1617/s11527-018-1275-z.

Bertolin, Chiara, Poorya Karvan, Andrea De Rosa, Nima Razavi, and Filippo Berto. 2021. "Relation between Fracture Characteristics and Moisture Content along Longitudinal Direction in a Naturally Drying Scots Pine." *Theoretical and Applied Fracture Mechanics* 112 (November 2020): 102911. https://doi.org/10.1016/j.tafmec.2021.102911.

Boadu, K. B., Antwi-Boasiako, C., & Frimpong-Mensah, K. 2017. "Physical and Mechanical Properties of Klainedoxa Gabonensis with Engineering Potentia." *Journal of Forestry Research* 28 (3): 629–36.

CIFOR. 2014. "Priorités de Recherche Du CIFOR."

Ding, Z. H., M. Huang, and Z. R. Lu. 2016. "Structural Damage Detection Using Artificial Bee Colony Algorithm with Hybrid Search Strategy." *Swarm and Evolutionary Computation* 28: 1–13. https://doi.org/10.1016/j.swevo.2015.10.010.

Dourado, N, M F S F De Moura, J Xavier, and F A M Pereira. 2015. "A New Procedure for Mode I Fracture Characterization of Cement-Based Materials," 483–91. https://doi.org/10.1111/str.12165.

Engonga Edzang, A. C. S., Pambou Nziengui, C. F., Ekomy Ango, S., Ikogou, S., & Moutou Pitti, R. 2021. "Comparative Studies of Three Tropical Wood Species under Compressive Cyclic Loading and Moisture Content Changes." *Wood Material Science & Engineering* 16 (3): 196–203.

FAO. 2006. "Food and Agriculture Organization of the United Nations." *Global Forest Resources Assessment 2005: Progress towards Sustainable Forest Management.* FAO Forest.

Forsman, Karin, Maria Fredriksson, Erik Serrano, and Henrik Danielsson. 2021. "Moisture-Dependency of the Fracture Energy of Wood: A Comparison of Unmodified and Acetylated Scots Pine and Birch." *Holzforschung* 75 (8): 731–41. https://doi.org/10.1515/hf-2020-0174.

Frühmann. n.d. "Fracture Characteristics of Wood under Mode I, Mode II and Mode III Loading," no. November 2014: 37–41. https://doi.org/10.1080/01418610208240441.

Fu, J., H. Haeri, M. D. Yavari, V. Sarfarazi, M. F. Marji, and M. Guo. 2021. "A Linear Elastic Fracture Mechanics Analysis of the Pre-Cracked Concrete Failure Mechanism Under Modes I, II, III, and IV Loading Conditions." *Strength of Materials* 53 (5): 784–96. https://doi.org/10.1007/s11223-021-00344-5.

Fu, J. W., H. Haeri, V. Sarfarazi, and M. F. Marji. 2022. "Modeling the Ligament Breakage Mechanism in Concrete Specimens Using a Four-Point Bending Test." *Strength of Materials* 54 (4): 671–80. https://doi.org/10.1007/s11223-022-00445-9.

Fu, J.W., Li, T., Haeri, H. 2023. "Acoustic emission monitoring of crack growth from echelon notches using numerincal simulation." *Strength of Materials*, 55(1):128-145

Gérard, Jean., Daniel. Guibal, Sébastien. Paradis, and Jean-Claude. Cerre. 2017. *Tropical Timber Atlas: Technological Characteristics and Uses*.

Gérard, Jean, A Edi Kouassi, C Daigremont, P Détienne, D Fouquet, and M L B - Gerard1998 Vernay. 1998. *Synthèse Sur Les Caractéristiques Technologiques de Référence Des Principaux Bois Commerciaux Africains*. CIRAD-forêt.

Gomes, Guilherme Ferreira, Yohan Alí Diaz Mendéz, Sebastião Simões da Cunha, and Antônio Carlos Ancelotti. 2018. "A Numerical–Experimental Study for Structural Damage Detection in CFRP Plates Using Remote Vibration Measurements." *Journal of Civil Structural Health Monitoring* 8 (1): 33–47. https://doi.org/10.1007/s13349-017-0254-3.

Grandgirard, Julie, Denis Poinsot, Liliane Krespi, Jean Pierre Nénon, and Anne Marie Cortesero. 2002. "Costs of Secondary Parasitism in the Facultative Hyperparasitoid Pachycrepoideus Dubius: Does Host Size Matter?" *Entomologia Experimentalis et Applicata* 103 (3): 239–48. https://doi.org/10.1023/A.

Grédiac, M., & Hild, F. (Eds.). (2012). *Full-field measurements and identification in solid mechanics*. John Wiley & Sons.

Gross, B., & Srawley, J. E. 1965. "Stress-Intensity Factors for Single-Edge-Notch Specimens in Bending or Combined Bending and Tension by Boundary Collocation of a Stress Function." *National Aeronautics and Space Administration.* 2603.

Hassan Vand, Mojtaba, Jan Tippner, and Martin Brabec. 2023. "Effects of Species and Moisture Content on the Behaviour of Solid Wood under Impact." *European Journal of Wood and Wood Products*, no. 2015. https://doi.org/10.1007/s00107-023-01986-9.

Irwin, G. R. 1958. "Discussion of the Dynamic Stress Distribution Surrounding a Running Crack-A Photoelastic Analysis." *In SESA Proc* Vol. 16: 93–96.

J.W.Fu, T.Li, and H. Haeri. 2023. "ACOUSTIC EMISSION MONITORING OF CRACK GROWTH FROM ECHELON NOTCHES USIN NUMERICAL SIMULATION."

Jozsa, L. A., & Middleton, G. R. 1994. "A Discussion of Wood Quality Attributes and Their Practical Implications."

Jungstedt, Erik, Sören Östlund, and Lars A. Berglund. 2022. "Transverse Fracture Toughness of Transparent Wood Biocomposites by FEM Updating with Cohesive Zone Fracture Modeling." *Composites Science and Technology* 225 (July): 109492. https://doi.org/10.1016/j.compscitech.2022.109492.

Konukcu, Arif C, Izmir Katip, and Celebi Universitesi. 2022. "Determination of Mode I Fracture Behavior of Southern Yellow Pine (Pinus Taeda L .) Wood Using Single-Edge-Notched Bending Test," no. April. https://doi.org/10.37763/wr.1336-4561/67.2.280290.

Konukcu, Arif Caglar. 2022. "Fracture Behavior of Wood Under Mode I Loading in Tangential Direction." *Drvna Industrija* 73 (4): 445–52. https://doi.org/10.5552/drvind.2022.2135.

Konukcu, Arif Caglar, Franklin Quin, and Jilei Zhang. 2021. "Effect of Growth Rings on Fracture Toughness of Wood." *European Journal of Wood and Wood Products* 79 (6): 1495–1506. https://doi.org/10.1007/s00107-021-01738-7.

Kurul, Fatih, and Hizir Volkan Görgün. 2022. "EFFECT OF THERMAL MODIFICATION ON SOME PHYSICAL AND MECHANICAL PROPERTIES OF YELLOW POPLAR (Liriodendron Tulipifera)."

Drewno 65 (209). https://doi.org/10.12841/wood.1644-3985.380.01.

Luimes, R. A., A. S.J. Suiker, C. V. Verhoosel, A. J.M. Jorissen, and H. L. Schellen. 2018. "Fracture Behaviour of Historic and New Oak Wood." *Wood Science and Technology* 52 (5): 1243–69. https://doi.org/10.1007/s00226-018-1038-6.

Maaß, Mona-christin, Salimeh Saleh, Holger Militz, and Cynthia A Volkert. 2020. "The Structural Origins of Wood Cell Wall Toughness" 1907693. https://doi.org/10.1002/adma.201907693.

Majano Majano, M. Almudena, Mark Hughes, and José L. Fernández-Cabo. 2010. "A Fracture Mechanics Study of Thermally Modified Beech for Structural Applications." *11th World Conference on Timber Engineering 2010, WCTE 2010* 3 (November 2014): 2103–8.

Mall, By S., and and James E. Shottafer Joseph F. Murphy, M. ASCE. 1983. "Criterion for Mixed Mode Fracture in Wood" 109 (3): 680–90.

Maria, Cicilia, Erna Susanti, Tetsuya Nakao, and Hiroshi Yoshihara. 2010. "Examination of the Failure Behaviour of Wood with a Short Crack in the Tangential – Radial System by Single-Edge-Notched Bending Test." *Engineering Fracture Mechanics* 77 (13): 2527–36. https://doi.org/10.1016/j.engfracmech.2010.05.019.

Merhar, Miran, Rostand Moutou Pitti, and Tom Argensse. 2023. "Mode I Fracture Properties of Thermally-Modified Spruce Wood (Picea Abies) at Different Moisture Contents." *Wood Material Science and Engineering* 18 (6): 2093–2103. https://doi.org/10.1080/17480272.2023.2228280.

Moura, M F S F De, and N Dourado. 2018. "Mode I Fracture Characterization of Wood Using the TDCB Test." *Theoretical and Applied Fracture Mechanics* 94 (December 2017): 40–45. https://doi.org/10.1016/j.tafmec.2018.01.005.

Nakao, Tetsuya, Cicilia Maria, and Erna Susanti. 2012. "Examination of the Failure Behavior of Wood with a Short Crack in the Radial – Longitudinal System by Single-Edge-Notched Bending Test," 453–58. https://doi.org/10.1007/s10086-012-1266-6.

NF B51- 004. 1985. "Bois - Détermination de l'humidité." *Afnor*, 8.

NF B51-005. 1985. "Détermination de La Masse Volumique." *Afnor*, 8.

NF B51 - 008. 2017. "Essai de Flexion Statique - Détermination de La Résistance à La Flexion Statique de Petites Éprouvettes sans Défauts." *Afnor*, 20.

Nziengui, C. P., Turesson, J., Odounga, B. 2018. "Détermination Des Principales Caractéristiques Physiques et Mécaniques Du Sapin Blanc Du Massif Central et de l ' Okoumé Du Gabon .," no. May.

Odounga, Bernard, Moutou Pitti, Evelyne Toussaint, and Michel Grédiac. 2019. "Mixed Mode Fracture of Some Tropical Species with the Grid Method." *Engineering Fracture Mechanics*, no. January: 0–1. https://doi.org/10.1016/j.engfracmech.2019.04.018.

Odounga, Bernard, Evelyne Toussaint, and Michel Grédiac. 2018. "Mode I Fracture of Tropical Woods Using Grid Method." *Theoretical and Applied Fracture Mechanics* 95 (January): 1–17. https://doi.org/10.1016/j.tafmec.2018.02.006.

Ostapska, Katarzyna, and Kjell Arne Malo. 2020. "Wedge Splitting Test of Wood for Fracture Parameters

445 Estimation of Norway Spruce." *Engineering Fracture Mechanics*, no. March: 107024.
446 https://doi.org/10.1016/j.engfracmech.2020.107024.
447 Phan, Ngoc Anh, Myriam Chaplain, Stéphane Morel, and Jean Luc Coureau. 2017. "Influence of Moisture
448 Content on Mode I Fracture Process of Pinus Pinaster: Evolution of Micro-Cracking and Crack-Bridging
449 Energies Highlighted by Bilinear Softening in Cohesive Zone Model." *Wood Science and Technology* 51
450 (5): 1051–66. https://doi.org/10.1007/s00226-017-0907-8.
451 Ravenshorst, G. J. P., Gard, W. F. and van de Kuilen, J. W. G. 2013. "The Importance of Characterisation and
452 Sampling of Tropical Wood Species with Regard to Strength and Durability Classification." *HERON* 58
453 (2/3): 195–222.
454 Reiterer, A., & Tschegg, S. 2002. "The Influence of Moisture Content on the Mode I Fracture Behaviour of
455 Sprucewood," no. January. https://doi.org/10.1023/A.
456 Reiterer, A, and G Sinn. 2002. "Fracture Characteristics of Different Wood Species under Mode I Loading
457 Perpendicular to the Grain Fracture Characteristics of Different Wood Species under Mode I Loading
458 Perpendicular to the Grain" 5093 (September 2017). https://doi.org/10.1016/S0921-5093(01)01721-X.
459 Romanowicz, Marek. 2022. "Numerical Assessment of the Apparent Fracture Process Zone Length in Wood
460 under Mode I Condition Using Cohesive Elements." *Theoretical and Applied Fracture Mechanics* 118
461 (April): 103229. https://doi.org/10.1016/j.tafmec.2021.103229.
462 Simpson, William T. 1991. "Dry Kiln Operator ' s Manual Dry Kiln Operator ' s Manual Edited by," no. 188:
463 41.
464 Stanzl-Tschegg, S. 2006. "Microstructure and Fracture Mechanical Response of Wood," no. May.
465 https://doi.org/10.1007/s10704-006-0052-0.
466 Stanzl-Tschegg, S. E. 2006. "Microstructure and Fracture Mechanical Response of Wood," no. June 2006.
467 https://doi.org/10.1007/s10704-006-0052-0.
468 Wang, Q., L. J. Sun, D. C. Wang, J. W. Fu, C. L. Guo, and H. Haeri. 2023. "Particle Flow Modeling for the
469 Crack Growth Analysis of Non-Persistent Cracks." *Strength of Materials* 55 (2): 371–83.
470 https://doi.org/10.1007/s11223-023-00531-6.
471 Yin, Xing, Qinghua Li, Qingmin Wang, Hans Wolf Reinhardt, and Shilang Xu. 2023. "The Double-K Fracture
472 Model: A State-of-the-Art Review." *Engineering Fracture Mechanics* 277 (December).
473 https://doi.org/10.1016/j.engfracmech.2022.108988.
474 Yu, Ying, Ruixue Xin, Weihang Zeng, and Wen Liu. 2021. "Fracture Resistance Curves of Wood in the
475 Longitudinal Direction Using Digital Image Correlation Technique." *Theoretical and Applied Fracture*
476 *Mechanics* 114 (August): 102997. https://doi.org/10.1016/j.tafmec.2021.102997.
477 Zhou, Y., J. W. Fu, D. C. Wang, H. Haeri, L. J. Sun, and C. L. Guo. 2022. "Numerical Investigation of the
478 Influence of Circular Fillings on the Failure Mechanism in Samples Containing Nonpersistent Joints
479 Under Shear Loading Conditions." *Strength of Materials* 54 (5): 880–88. https://doi.org/10.1007/s11223-
480 022-00465-5.
481 Zhu, Xian Kui, and James A. Joyce. 2012. "Review of Fracture Toughness (G, K, J, CTOD, CTOA) Testing

and Standardization." *Engineering Fracture Mechanics* 85: 1–46. https://doi.org/10.1016/j.engfracmech.2012.02.001.Q∑Q<

485 **Table 1**. Physical characteristics of the three species studied

Species	Properties			
	Water Content% (%)	Standard deviation	Basal density g/cm^3	Standard deviation
Padouk	19.14	7.32	0.83	0.05
Bilinga	22.10	9.67	0.73	0.03
Dabema	25.63	11.79	0.69	0.03

486

487 **Table 2**. Mechanical characteristics.

species	Properties					
	Young's modulus(MPa)	Standard deviation	Covariance% (%)	Bending stress (MPa)	Standard deviation	Covariance% (%)
Padouk	9905.29	601.09	1016.37	89.82	6.45	1016.37
Bilinga	9565.36	1112.7	821.28	81.68	16.74	821.28
Dabema	8392.31	2081.09	692.57	66.94	17.82	692.57

488

489 **Table 3**. Variation in energy parameters between three tropical woods

Designation	Number of samples tested per wood	Dabema	Bilinga	Padouk
*Energy recovery rate Gic(*j/m²)				
a = 0 mm	05	(1612.10 ±623.21)^{ab}	(1747.91 ±520.14)^{a}	(2958.63 ±918.92)^{a}
a = 4 mm	05	(885.87±401.96)^{ab}	(989.63 ±694.11)^{a}	(2231.14±1272.14)^{a}
a = 8 mm	05	(581.11±226.91)^{a}	(519.72 ±91.46)^{a}	(490.61±201.28)^{a}
*Stress intensity factor Kic(MPa*m$^{1/2}$)*				
a = 4 mm	05	(1.29 ±0.38)^{a}	(1.51 ±0.42)^{a}	(2.41±0.90)^{a}
a = 8 mm	05	(0.98±0.44)^{a}	(1.28 ±0.39)^{a}	(1.10±0.20)^{a}
Flexural stress σ_n (MPa)				
a = 0 mm	05	(66.94±17.82)^{a}	(81.68 ±16.74)^{a}	(89.82 ±6.45)^{a}
a = 4 mm	05	(37.15±11.08)^{b}	(43.46±11.98)ab	(69.34 ±25.94)^{a}
a = 8 mm	05	(16.78 ±7.56)^{a}	(21.85±6.56)^{a}	(18.77 ±3.47)^{a}

490 The same letter in the subscript indicates that the mean values provided by each wood for the same primer
491 value are not significantly different at the significance level α = 0.05 (Tukey test).
492

493 **Table 4.** Results of the analysis of variance testing the effect of fracture parameters (wood species, crack
494 length) on cracking resistance

Designation	Number of samples tested per wood	Dabema	Bilinga	Padouk
*Energy recovery rate Gic(*j/m²)				
a = 0 mm	05	(1612.096± 623)[a]	(1747.912±520.14)[b]	(2958.626± 918)[b]
a = 4 mm	05	(885.872 ±401.9)[ab]	(989.63±694)[ab]	(2231.136± 1272)[b]
a = 8 mm	05	(581.108± 226.91)[a]	(519.72±91.47)[a]	(490.610 ± 201)[a]
Pvalue		(0.00968)	(0.00746)	(0.00319)
*Stress intensity factor Kic(MPa*m$^{1/2}$)*				
a = 4 mm	05	(288± 0.383)[a]	(1.506± 0.416)[a]	2.406 ±0.9)[b]
a = 8 mm	05	(0.982± 0.441)[a]	(1.280± 0.385)[a]	1.098 ±0.2)[a]
Pvalue		(0.276)	(0.399)	(0.0134)
Flexural stress σ_n (MPa)				
a = 0 mm	05	(66.938± 17.817)[b]	(81.68± 16.73)[c]	89,82 (6,45)[b]
a = 4 mm	05	(37.148 ±11)[a]	(43.46± 11.98)b	69.34 (25.94)[b]
a = 8 mm	05	(16.778 ± 7.554)[a]	(21.85 ± 6.55)[a]	18.77 (3.47)[a]
Pvalue		(0.000182)	(0.0000233)	0.0000323

495

Figure captions

Figure 1. (A) Billets and quaterlots of the species used, (B) Procedure for cutting the specimens; (C) specimens of the three species of wood.

Figure 2. A) External view of the oven; B) Weighing of our test specimens.

Figure 3. Kinematic diagram of the bending test device consisting of the following elements:1. Elastic ring, 2. Digital comparator, 3. Force, 4Fixed support,5. Digital comparator, 6 Comparator support lever, 7 Hand wheel, 8. Comparator fixed support, 9. lever rotation speed indicator, 10. frame, 11. test tube, 12. plate and 13. piston.

Figure 4. The general configuration of the test set-up for the SENB test (S=320, B=20, W=20)

Figure 5. Representative load-displacement curves for the different primer values and for each wood: (a) Padouk, (b) Bilinga and (c) Dabema.

Figure 6. Failure of specimens in mode I

Figure 7. Typical tangential structure profiles of three wood species showing fibre orientation and microstructure Padouk (a), Dabema(b) and Bilinga(c).

Figure 8. Distribution of the energy restitution rate, the stress intensity factor and the average and maximum stress resistance of the three groups: A0 specimens without notches; A1 specimens with 4mm deep notches and A2 specimens with 8mm notches.

Figure 9. Comparison of the amplitudes of the energy restitution rate (Gic) of three different lengths of primers on the Padouk, Bilinga and Dabema specimens.

Figure 10. Effects on the amplitude of the energy restitution rate *Gic* and the stress intensity factor *Kic* (their maximum values) of Padouk, Bilinga and Dabema specimens as a function of the density of each species. (a_0) denotes the initiation length.

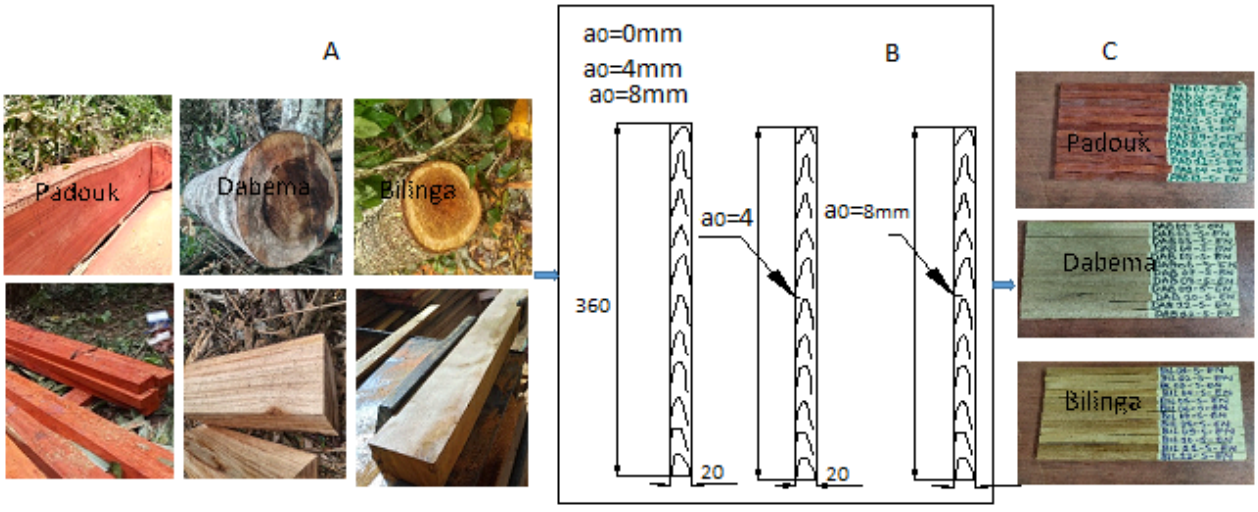

519 **Figure 1.**

520

521 **Figure 2.**

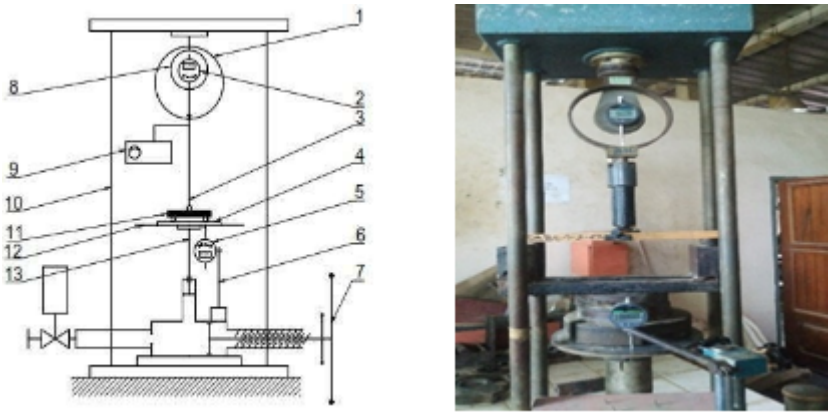

522

523 **Figure 3.**

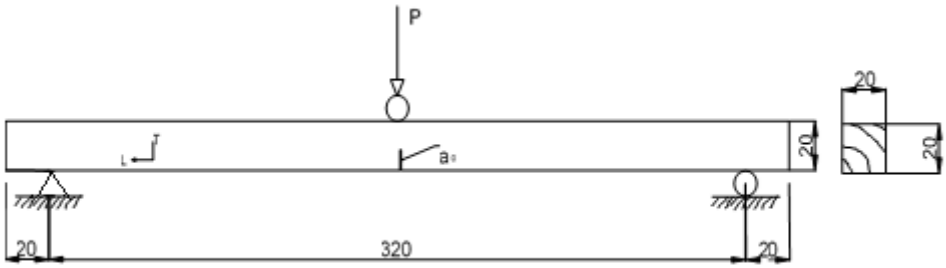

524

525 **Figure 4.**

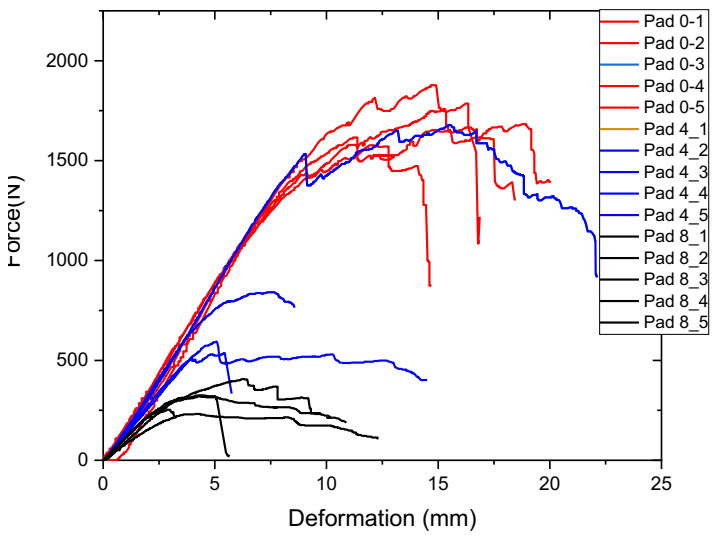

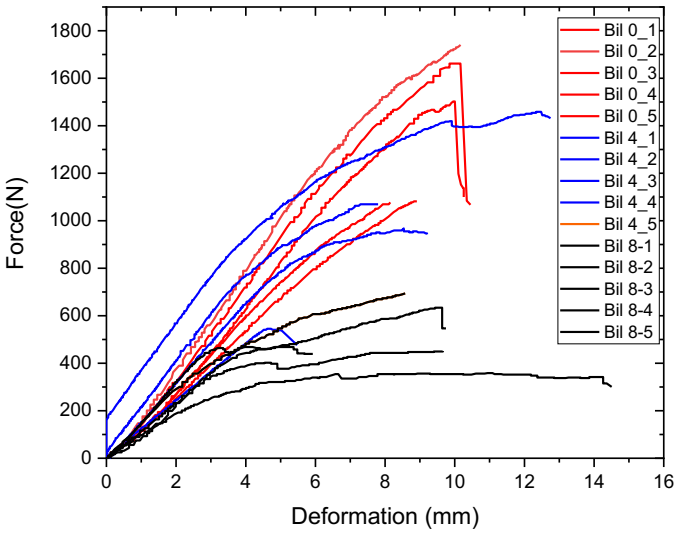

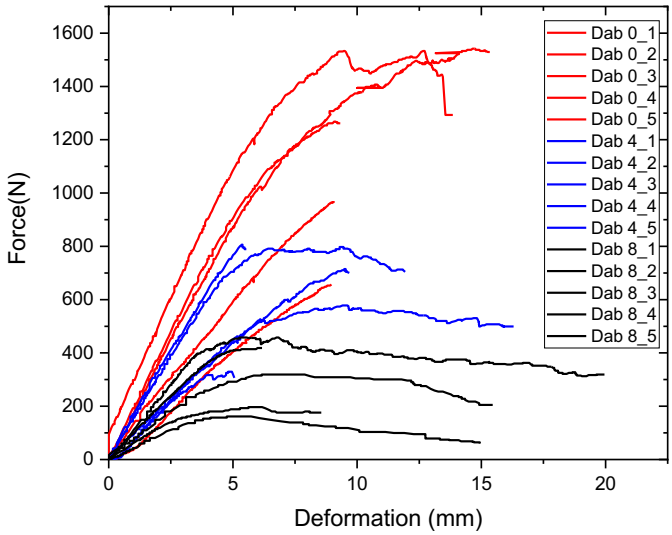

526 **Figure 5.**

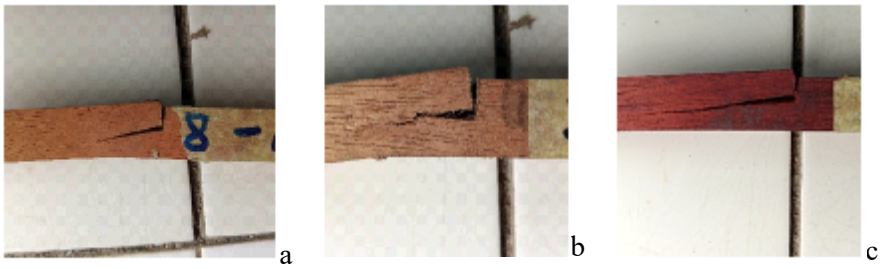

Bilinga Dabema Padouk

527

528 **Figure 6.**

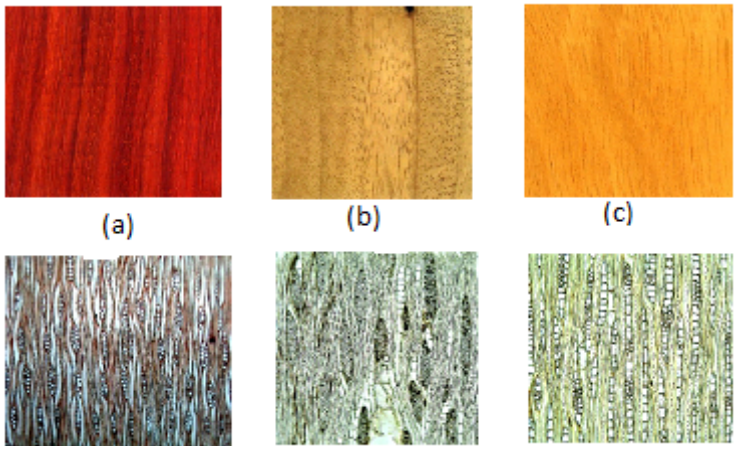

529

530 **Figure 7.**

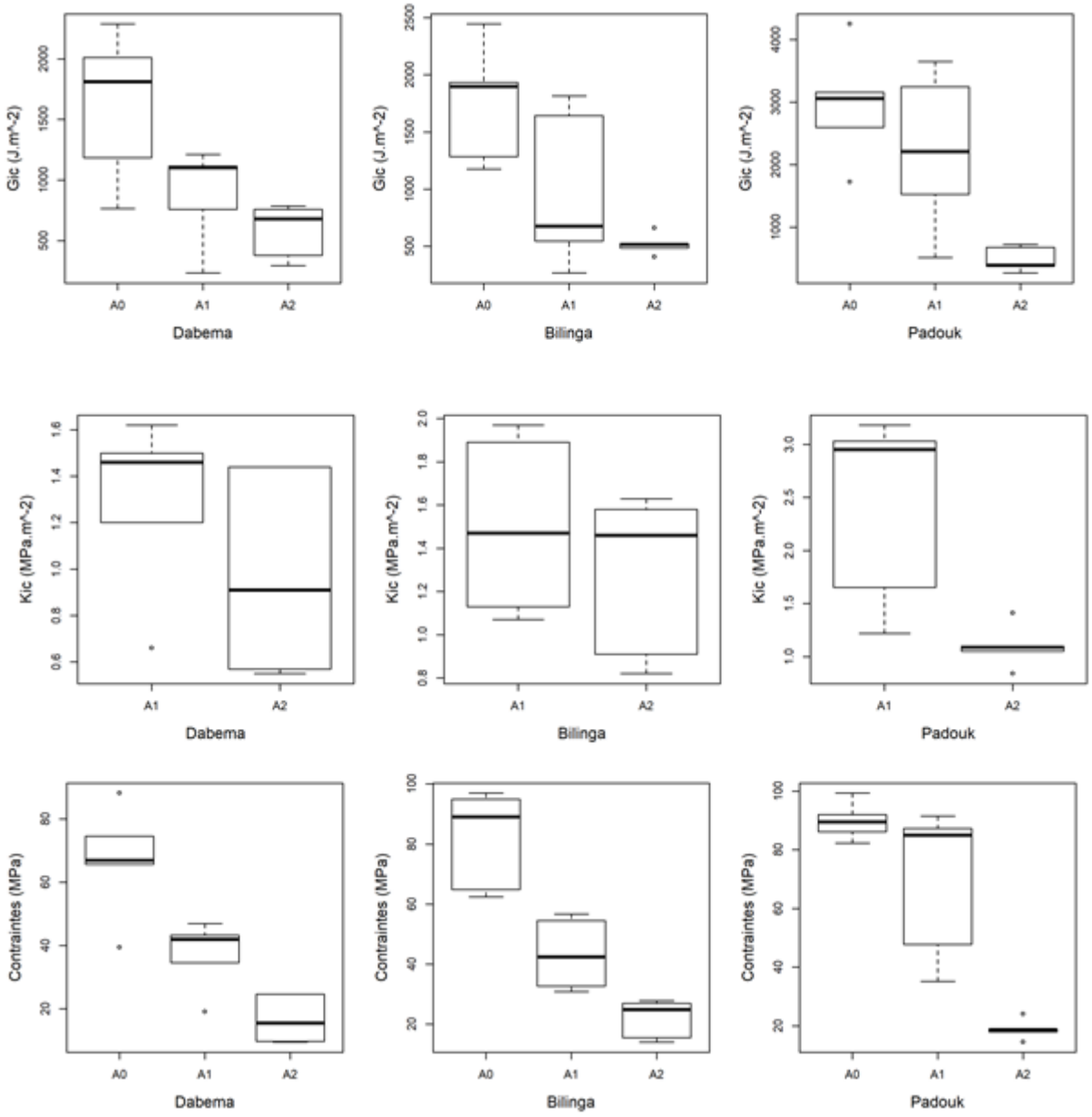
Gic (J.m^-2)
Dabema
Billinga
Padouk
Kic (MPa.m^-2)
Contraintes (MPa)
A0
A1
A2

531 **Figure 8.**

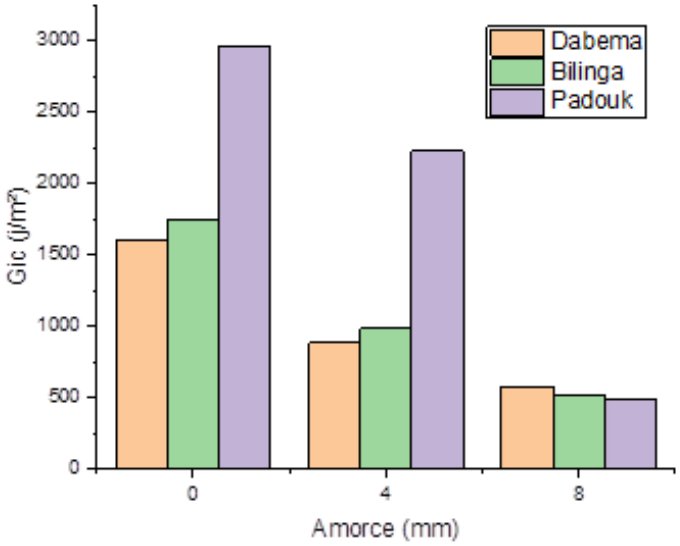

532

533 **Figure 9.**

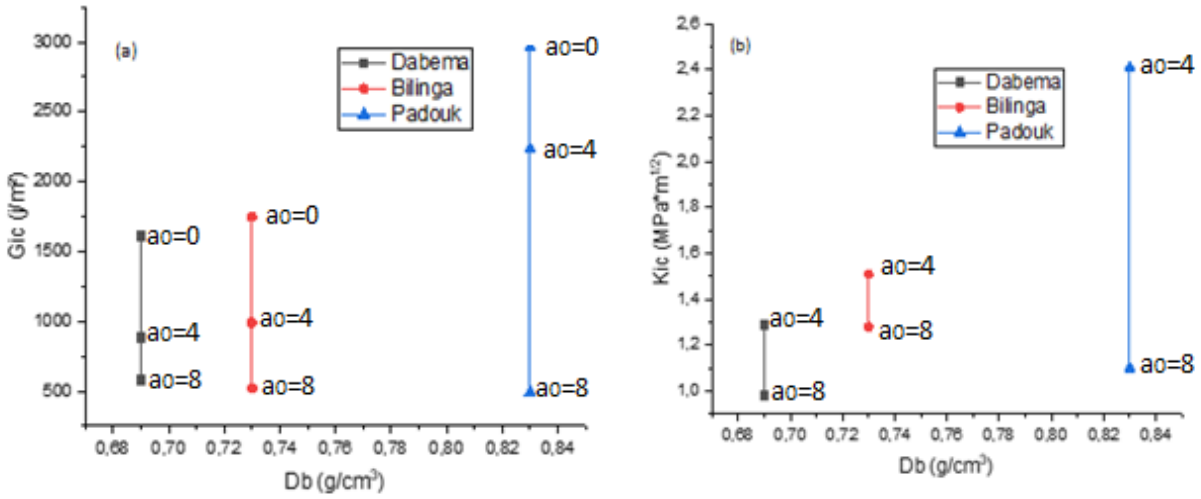

534 **Figure 10.**